

# High-temperature thermoelectric properties of the $\beta$ -As<sub>2-x</sub>Bi<sub>x</sub>Te<sub>3</sub> solid solution

Cite as: APL Mater. 4, 104901 (2016); <https://doi.org/10.1063/1.4950947>

Submitted: 04 April 2016 . Accepted: 03 May 2016 . Published Online: 01 June 2016

J.-B. Vaney, G. Delaizir, A. Piarristeguy, J. Monnier, E. Alleno, E. B. Lopes, A. P. Gonçalves, A. Pradel, A. Dauscher, C. Candolfi, and B. Lenoir



View Online



Export Citation



CrossMark

## ARTICLES YOU MAY BE INTERESTED IN

[Characterization of Lorenz number with Seebeck coefficient measurement](#)


APL Materials 3, 041506 (2015); <https://doi.org/10.1063/1.4908244>

[Analysis of the temperature dependence of the thermal conductivity of insulating single crystal oxides](#)

APL Materials 4, 104815 (2016); <https://doi.org/10.1063/1.4966220>

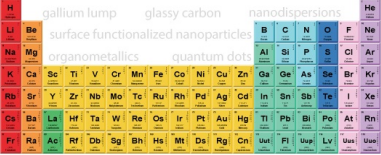
[Thermoelectric properties of n-type SrTiO<sub>3</sub>](#)

APL Materials 4, 104803 (2016); <https://doi.org/10.1063/1.4952610>



**AMERICAN ELEMENTS**

THE ADVANCED MATERIALS MANUFACTURER®



additive manufacturing epitaxial crystal growth cerium oxide polishing powder silver nanoparticles sputtering targets III-IV semiconductors CVD precursors europium phosphors

gallium lump glassy carbon nanodispersions InAs wafers laser crystals ultra high purity materials MOFs

surface functionalized nanoparticles organometallics quantum dot Al Si P S Cl Ar Na

deposition slugs OLED Lighting spintronics solar energy osmium nanoribbons thin films chalcogenides AuNP

GDC Li-ion battery electrolytes 99.999% ruthenium spheres Cs Ba La Hf Ta W Re Os Ir Pt Au Hg Tl Pb Bi Po At Rn

endohedral fullerenes copper nanoparticles diamond micropowder CIGS MBE grade materials palladium catalysts flexible electronics YBCO

pyrolytic graphite 3d graphene foam indium tin oxide mesoporous silica beta-barium borate borosilicate glass dysprosium pellets InGaAs

raman substrates sapphire windows tungsten carbide InGaAs

barium fluoride carbon nanotubes lithium niobate scandium powder

perovskite crystals yttrium iron garnet alternative energy h-BN

gold nanocubes graphene oxide macromolecules photonics

rhodium sponge fiber optics beamsplitters infrared dyes zeolites

fused quartz metallocenes platinum ink buckyballs Ti-6Al-4V

**Now Invent.™**

The Next Generation of Material Science Catalogs

[www.americanelements.com](http://www.americanelements.com)



## High-temperature thermoelectric properties of the $\beta$ -As<sub>2-x</sub>Bi<sub>x</sub>Te<sub>3</sub> solid solution

J.-B. Vaney,<sup>1</sup> G. Delaizir,<sup>2</sup> A. Piarristeguy,<sup>3</sup> J. Monnier,<sup>4</sup> E. Alleno,<sup>4</sup> E. B. Lopes,<sup>5</sup> A. P. Gonçalves,<sup>5</sup> A. Pradel,<sup>3</sup> A. Dauscher,<sup>1</sup> C. Candolfi,<sup>1</sup> and B. Lenoir<sup>1,a</sup>

<sup>1</sup>Institut Jean Lamour, UMR 7198 CNRS–Université de Lorraine, Nancy, France

<sup>2</sup>Science des Procédés Céramiques et de Traitements de Surface (SPCTS), UMR CNRS 7315–Université de Limoges, Limoges, France

<sup>3</sup>Institut Charles Gerhardt (ICG), UMR 5253 CNRS–Université de Montpellier, Montpellier, France

<sup>4</sup>Institut de Chimie et des Matériaux Paris Est (ICMPE), UMR 7182 CNRS–Université Paris-Est Créteil, Thiais, France

<sup>5</sup>C2TN, Instituto Superior Técnico, Universidade de Lisboa, Lisboa, Portugal

(Received 4 April 2016; accepted 3 May 2016; published online 1 June 2016)

Bi<sub>2</sub>Te<sub>3</sub>-based compounds are a well-known class of outstanding thermoelectric materials.  $\beta$ -As<sub>2</sub>Te<sub>3</sub>, another member of this family, exhibits promising thermoelectric properties around 400 K when appropriately doped. Herein, we investigate the high-temperature thermoelectric properties of the  $\beta$ -As<sub>2-x</sub>Bi<sub>x</sub>Te<sub>3</sub> solid solution. Powder X-ray diffraction and scanning electron microscopy experiments showed that a solid solution only exists up to  $x = 0.035$ . We found that substituting Bi for As has a beneficial influence on the thermopower, which, combined with extremely low thermal conductivity values, results in a maximum  $ZT$  value of 0.7 at 423 K for  $x = 0.017$  perpendicular to the pressing direction. © 2016 Author(s). All article content, except where otherwise noted, is licensed under a Creative Commons Attribution (CC BY) license (<http://creativecommons.org/licenses/by/4.0/>). [<http://dx.doi.org/10.1063/1.4950947>]

The efficiency with which thermoelectric materials convert a thermal gradient into electricity and vice-versa at an operating temperature  $T$ , is governed by the dimensionless figure of merit  $ZT = \alpha^2 T / (\kappa_e + \kappa_L)$ .<sup>1,2</sup> High  $ZT$  values are synonymous with high efficiency and are achieved in materials exhibiting a fine balance between the thermopower  $\alpha$ , the electrical resistivity  $\rho$ , and the electronic and lattice thermal conductivities,  $\kappa_e$  and  $\kappa_L$ , respectively.<sup>1,2</sup> Heavily doped semiconductors with carrier concentrations ranging from  $10^{19}$  to  $10^{21}$  cm<sup>-3</sup> and crystallizing with a complex unit cell usually achieve the best compromise between these three transport properties.<sup>1,2</sup>

Depending on the synthesis conditions, the polymorphic compound As<sub>2</sub>Te<sub>3</sub> crystallizes with either monoclinic (space group  $C2/m$ ) or rhombohedral symmetry (space group  $R\bar{3}m$ ), referred to as the  $\alpha$  and  $\beta$  form, respectively.<sup>3–7</sup>  $\alpha$ -As<sub>2</sub>Te<sub>3</sub> undergoes several phase transitions at high pressures driving this insulator into a semi-metallic phase before eventually entering a metallic regime.<sup>8</sup> At ambient pressure,  $\beta$ -As<sub>2</sub>Te<sub>3</sub> transforms into the  $\alpha$  form above 473 K and undergoes a subtle lattice distortion near 190 K that breaks the rhombohedral symmetry and leads to a novel monoclinic unit cell exhibiting a fourfold modulation along the  $b$  axis (named  $\beta'$ ).<sup>9</sup> Interestingly, both  $\alpha$ -As<sub>2</sub>Te<sub>3</sub> and  $\beta$ -As<sub>2</sub>Te<sub>3</sub> phases are semiconductors that meet the aforementioned requirements.<sup>10–14</sup> In particular, they share the remarkable feature of being poor thermal conductors with lattice thermal conductivities well below  $1 \text{ W m}^{-1} \text{ K}^{-1}$  above 300 K. Maximum  $ZT$  values of 0.8 at 523 K and 0.65 at 423 K were achieved in  $\alpha$ -As<sub>2</sub>Te<sub>3</sub> and  $\beta$ -As<sub>2</sub>Te<sub>3</sub>, respectively, using the substitution of Sn for As as a tuning parameter of the hole concentration.<sup>10,13</sup>

<sup>a</sup>Author to whom correspondence should be addressed. Electronic mail: [bertrand.lenoir@univ-lorraine.fr](mailto:bertrand.lenoir@univ-lorraine.fr)

The  $\beta$ -As<sub>2</sub>Te<sub>3</sub> compound is isostructural to the well-known Bi<sub>2</sub>Te<sub>3</sub>-based thermoelectric materials used in solid-state cooling applications.<sup>1,2</sup> First reported as a high-pressure phase,<sup>7</sup> polycrystalline samples could be obtained with high purity by conventional melting-quenching techniques allowing for a detailed investigation of its transport properties and of the influence of substitution on either the As or Te site.<sup>10</sup> Our prior work on Sn-substituted  $\beta$ -As<sub>2</sub>Te<sub>3</sub> has provided hints at the presence of defects in this material,<sup>10</sup> akin to the Bi<sub>2</sub>Te<sub>3</sub>-based alloys where defect chemistry plays a central role in determining the thermoelectric performances.<sup>1,2</sup> In addition, this compound has been suggested to harbor topological insulating properties when an uniaxial strain is applied along the *c* axis,<sup>14,15</sup> which could be experimentally realized by applying either an external pressure or a chemical pressure through substitutions.

Despite the large number of isovalent and aliovalent substitutions that can be envisaged, alloying  $\beta$ -As<sub>2</sub>Te<sub>3</sub> with isostructural Bi<sub>2</sub>Te<sub>3</sub> appears as a natural route to further improve the *ZT* values in this family. The possibility to form a solid solution between these two compounds is of particular interest for both practical and fundamental reasons. Continuously varying the As/Bi ratio could act as a tuning parameter of the spin-orbit coupling that would give rise to a transition from a trivial band insulator to a topological insulator, as observed, for instance, in the Pb<sub>1-x</sub>Sn<sub>x</sub>Se or TlBiSe<sub>2-x</sub>S<sub>x</sub> systems.<sup>16-19</sup> On a more practical point of view, alloying with Bi may help to increase the power factor of  $\beta$ -As<sub>2</sub>Te<sub>3</sub> and to push the maximum *ZT* values of  $\beta$ -As<sub>2</sub>Te<sub>3</sub> closer to room temperature.

Our preliminary investigation of the low-temperature thermoelectric properties of the  $\beta$ -As<sub>2-x</sub>Bi<sub>x</sub>Te<sub>3</sub> compounds has revealed that Bi helps to decrease the electrical resistivity without being at the expense of a significant increase in the thermal conductivity.<sup>12</sup> Remarkably, the *ZT* values achieved at 300 K were similar to those measured in Sn-substituted samples, suggesting that interesting thermoelectric performances could be obtained at higher temperatures.<sup>12</sup> Herein, we extend these investigations with a detailed study of the thermoelectric properties at moderately high temperatures (300–423 K) of polycrystalline  $\beta$ -As<sub>2-x</sub>Bi<sub>x</sub>Te<sub>3</sub> samples in the homogeneity range. The substitution of Bi for As results in a significant increase in the *ZT* values with respect to the unsubstituted phase  $\beta$ -As<sub>2</sub>Te<sub>3</sub> with a peak *ZT* of 0.7 at 423 K for *x* = 0.017 perpendicular to the pressing direction.

All synthetic procedures were carried out in a dry, argon-filled glove box. Caution is required for preparing and handling samples made with arsenic and for their disposal. More specifically, the As vapor pressure may become significant at high temperatures thereby possibly resulting in an explosion of the quartz tube and releasing toxic As vapor. Polycrystalline  $\beta$ -As<sub>2-x</sub>Bi<sub>x</sub>Te<sub>3</sub> samples (*x* = 0.0, 0.015, 0.025, 0.035, 0.1, 0.2) were prepared by direct reactions of stoichiometric quantities of pure elements (99.99% As Goodfellow, 99.999% Te 5N+ and 99.9999% Bi 5N+, all in shots). The mixtures were loaded in quartz tubes sealed under secondary vacuum and heated up to 923 K at a rate of 10 K min<sup>-1</sup>. The tubes were maintained at this temperature for 2 h before being quenched in icy water. The resulting ingots were ground into fine powders and consolidated at room temperature under a pressure of 750 MPa yielding dense cylindrical pellets (~10 mm in diameter and ~7 mm in thickness). No further annealing step has been applied to the pellets after consolidation. The remarkable mechanical properties of this family of compounds led to geometric densities higher than 95% of the theoretical densities.

The phase purity and crystal structure were verified by powder X-ray diffraction (PXRD) using a Bruker D8 Advance diffractometer (CuK $\alpha$ <sub>1</sub> radiation). The lattice parameters were determined at 300 K by Rietveld refinements of the PXRD patterns using the Fullprof software (Table I). The chemical homogeneity and spatial distribution of the elements were assessed by scanning electron microscopy (SEM) and energy dispersive X-ray spectroscopy (EDXS) using a Quanta FEG (FEI). The chemical compositions were determined by electron probe microanalysis (EPMA) on mirror-polished surface of bulk pieces with a JEOL JXA 8530F instrument equipped with wavelength-dispersive spectrometers.  $\beta$ -As<sub>2</sub>Te<sub>3</sub> and Bi were used as standards to determine the As, Te, and Bi contents. The binary  $\beta$ -As<sub>2</sub>Te<sub>3</sub> compound was used to lower the mismatch between these samples and other As and Te standards owing to differing chemical environments of these elements. Because the absence of secondary phases in  $\beta$ -As<sub>2</sub>Te<sub>3</sub> was confirmed by EDXS analyses, this sample was considered as stoichiometric for these measurements. With these standards, the total weight

TABLE I. Nominal and actual compositions measured by EPMA on the polycrystalline series  $\beta$ -As<sub>2-x</sub>Bi<sub>x</sub>Te<sub>3</sub>. The compositions have been normalized to five atoms per formula unit. The lattice parameters ( $a$  and  $c$ ) were determined from Rietveld refinements against PXRD patterns collected at 300 K. The Hall carrier concentration ( $p_H$ ) and the Hall mobility ( $\mu_H$ ) measured at 300 K in samples cut perpendicular to the pressing direction are also mentioned.

Nominal composition	EPMA	$a$ (Å), $c$ (Å)	$p_H$ ( $10^{19}$ cm <sup>-3</sup> )	$\mu_H$ (cm <sup>2</sup> V <sup>-1</sup> s <sup>-1</sup> )
As <sub>2</sub> Te <sub>3</sub>	As <sub>1.985</sub> Te <sub>3.015</sub>	4.0473(2), 29.502(3)	8.4	48.6
As <sub>1.985</sub> Bi <sub>0.015</sub> Te <sub>3</sub>	As <sub>1.995</sub> Bi <sub>0.017</sub> Te <sub>2.988</sub>	4.0503(2), 29.538(2)	7.1	81.2
As <sub>1.975</sub> Bi <sub>0.025</sub> Te <sub>3</sub>	As <sub>1.980</sub> Bi <sub>0.024</sub> Te <sub>2.996</sub>	4.0518(2), 29.554(2)	6.8	69.5
As <sub>1.965</sub> Bi <sub>0.035</sub> Te <sub>3</sub>	As <sub>1.968</sub> Bi <sub>0.035</sub> Te <sub>2.997</sub>	4.0531(2), 29.566(1)	8.0	57.8

percentage of each analyzed point was between 99% and 101%. The chemical composition of each sample was obtained by averaging the atomic percentage of 90 different data points.

Owing to the anisotropy in the transport properties observed in Sn-substituted samples, the cold-pressed cylindrical pellets were cut into bar-, disc- or parallelepiped-shaped samples with a diamond wire saw both parallel and perpendicular to the pressing direction. The thermopower and electrical resistivity were measured simultaneously on bar-shaped samples between 300 and 423 K using a ZEM-3 (Ulvac-Riko) apparatus. The disc- or parallelepiped-shaped samples were utilized to measure the thermal diffusivity  $\alpha$  in the same temperature range using a Netzsch LFA 427 system. Thermal conductivity was calculated from the formula  $\kappa = \alpha C_p d$  where  $C_p$  is the specific heat and  $d$  is the experimental density. While the temperature dependence of  $d$  was neglected, the specific heat was measured from 300 to 423 K using a Netzsch Pegasus 404 apparatus. The combined uncertainty in the determination of the  $ZT$  values is estimated to be 17%.<sup>20</sup>

The crystal structure and phase purity of the  $\beta$ -As<sub>2-x</sub>Bi<sub>x</sub>Te<sub>3</sub> samples were confirmed by PXRD and SEM experiments. Figure 1 shows a representative Rietveld refinement of the PXRD pattern of the  $x = 0.017$  sample. Except for an additional reflection near  $2\theta = 31^\circ$  visible in all PXRD patterns

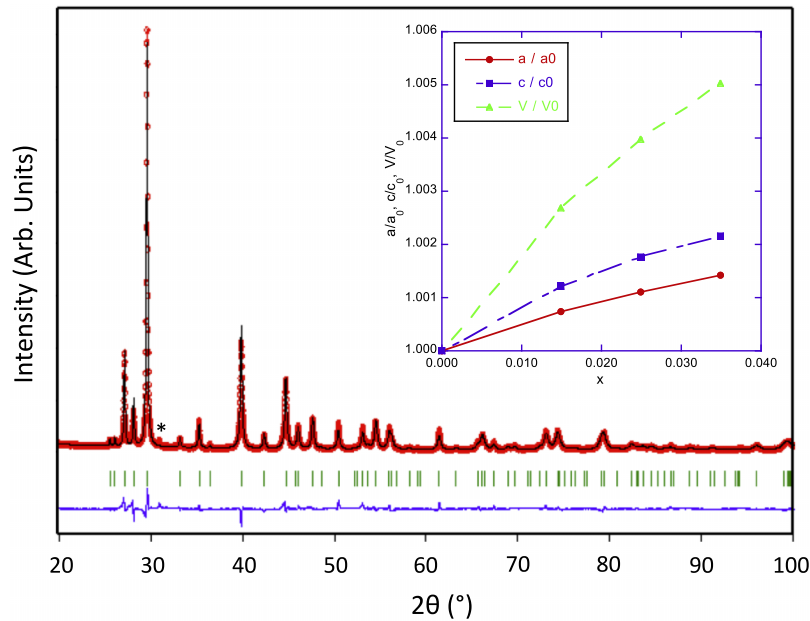


FIG. 1. Rietveld refinement of the representative PXRD pattern of the  $x = 0.017$  sample ( $R_B = 6.94$ ,  $\chi^2 = 6.94$ ). The asterisk marks the reflection ascribed to the AsTe impurity phase. The vertical green ticks mark the calculated reflection positions of the  $R\bar{3}m$  space group. The lowest blue line corresponds to the residuals of the refinement. The inset shows the evolution of the reduced hexagonal lattice parameters  $a/a_0$  and  $c/c_0$  determined at 300 K along with the reduced unit cell volume  $V/V_0$  as a function of the actual Bi content ( $a_0$ ,  $c_0$ , and  $V_0$  are the lattice parameters and volume of the binary sample  $\beta$ -As<sub>2</sub>Te<sub>3</sub>). The lines are guides to the eye. The errors related to the determination of the lattice parameters are smaller than the size of the symbols used.

and identified as the binary AsTe phase, no other secondary phases are visible for Bi contents up to  $x = 0.035$ . Above this concentration, additional reflections appear suggesting that  $\beta\text{-As}_{2-x}\text{Bi}_x\text{Te}_3$  is a solid solution up to only  $x = 0.035$ . SEM images collected in backscattering electron mode confirmed the phase-pure nature of the samples for  $x \leq 0.035$ .<sup>12</sup> Hence, only the chemical compositions and transport properties of single-phase samples ( $x \leq 0.035$ ) were subsequently studied. EPMA measurements confirmed the very good chemical homogeneity of the matrix and revealed an excellent correlation between the nominal and actual compositions (see Table I). Hereafter, we use the actual Bi content to label the samples.

The trends in the crystal structure upon alloying with Bi were determined by Rietveld refinements against PXRD data. The variations in the lattice parameters  $a$  and  $c$ , shown in the inset of Figure 1 as a function of the actual Bi content, indicate a monotonous expansion of the unit cell with  $x$  in agreement with the larger ionic radii of Bi with respect to As. Both parameters increase with  $x$  in a non-linear manner with a tendency to saturate at high Bi concentrations.

Figure 2(a) shows the evolution of  $\rho$  as a function of temperature as the Bi content varies from  $x = 0$  up to 0.035. The linear increase in the  $\rho$  values with temperature indicates that all samples have a metallic character. While all the samples share the common characteristic to exhibit significantly lower  $\rho$  in the perpendicular direction than in the parallel direction, the  $\rho$  values

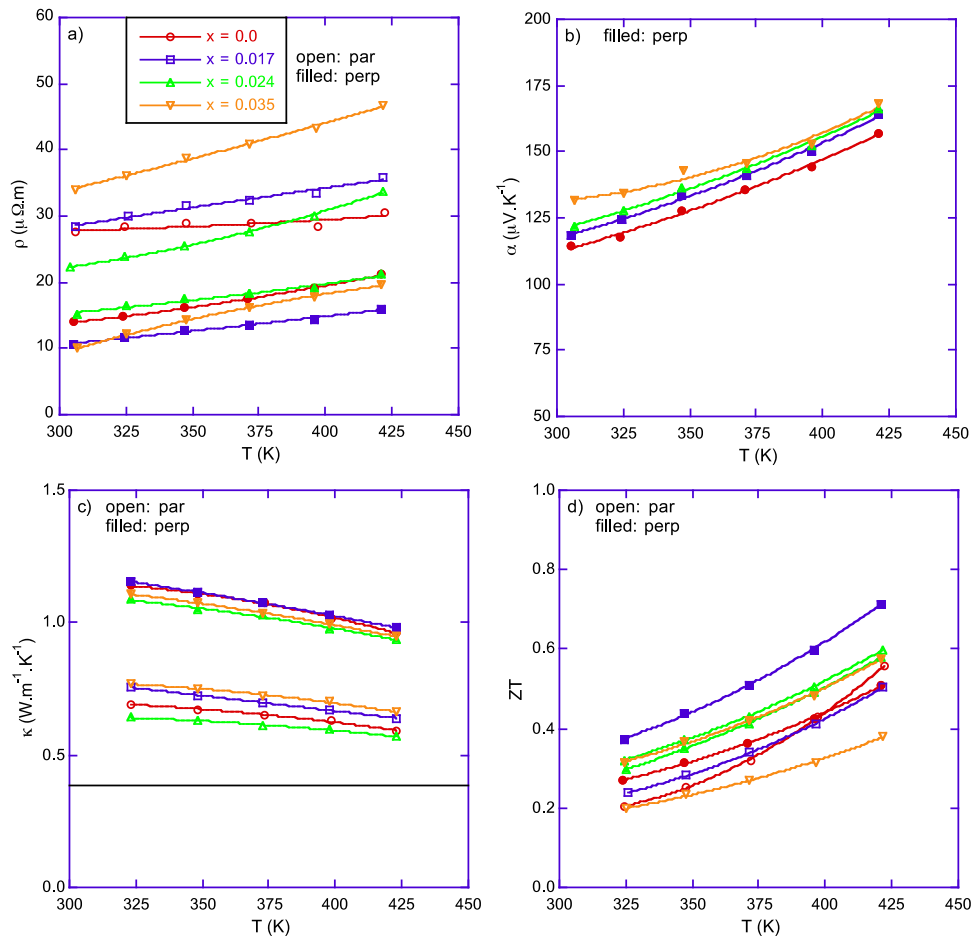


FIG. 2. Temperature dependence of the electrical resistivity  $\rho$  (a), thermopower  $\alpha$  (b), total thermal conductivity  $\kappa$  (c), and dimensionless thermoelectric figure of merit  $ZT$  (d). The lines are guides to the eye. The color-coded symbols are similar for all panels. The open and filled symbols refer to measurements performed parallel and perpendicular, respectively, to the pressing direction. For the sake of clarity, only the thermopower data taken in the perpendicular direction are shown in panel (b). In panel (c), the solid black line stands for the minimum thermal conductivity ( $0.38 \text{ W m}^{-1} \text{ K}^{-1}$ ) estimated from the longitudinal and transverse sound velocities (Ref. 13).

of the  $x = 0.017$  and  $0.035$  samples are lower than for  $x = 0.0$ . The fact that  $\rho$  does not evolve monotonically with  $x$  is tied to the non-monotonic variations in the Hall carrier concentration  $p_H$  and Hall mobility  $\mu_H$  revealed by Hall effect measurements (Table I).  $p_H$  first decreases from  $8.4 \times 10^{19} \text{ cm}^{-3}$  to  $6.8 \times 10^{19} \text{ cm}^{-3}$  on going from  $x = 0.0$  to  $0.024$  before increasing to  $8.4 \times 10^{19} \text{ cm}^{-3}$  for  $x = 0.035$ . Concomitantly,  $\mu_H$  increases from  $49 \text{ cm}^2 \text{ V}^{-1} \text{ s}^{-1}$  up to  $81 \text{ cm}^2 \text{ V}^{-1} \text{ s}^{-1}$  in the  $x = 0.017$  sample. Further alloying with Bi results in a gradual decrease in  $\mu_H$  to  $58 \text{ cm}^2 \text{ V}^{-1} \text{ s}^{-1}$  in the  $x = 0.035$  specimen. These results suggest that the activity of Bi as a dopant is non trivial and could reflect a strong influence of Bi atoms on the native defects induced by non-stoichiometry that exist in  $\beta\text{-As}_2\text{Te}_3$ , a situation similar to  $\text{Bi}_2\text{Te}_3$ -based materials where defect chemistry plays a prominent role.<sup>2,21</sup>

The linear dependence of  $\alpha(T)$ , shown in Figure 2(b), is consistent with the diffusive regime expected in metals and degenerate semiconductors. In contrast to  $\rho$ ,  $\alpha$  appears independent of the direction of the measurement to within experimental uncertainty with  $\alpha$  values varying from  $115 \text{ } \mu\text{V K}^{-1}$  at 300 K for  $x = 0.0$  up to  $170 \text{ } \mu\text{V K}^{-1}$  at 423 K for  $x = 0.035$ . The maximum  $\alpha$  values reached at 423 K are similar to those measured in the Sn-substituted series for similar hole concentrations.

The temperature dependence of the total thermal conductivity is shown in Figure 2(c). The electronic contribution to the thermal conductivity  $\kappa_e$  was calculated by the Wiedemann-Franz law  $\kappa_e = LT/\rho$  where the Lorentz number  $L$  determined for  $\beta\text{-As}_2\text{Te}_3$  ( $1.9 \times 10^{-8} \text{ V}^2 \text{ K}^{-2}$  at 300 K) has been considered.<sup>14</sup> Despite a limited structural complexity, the resulting lattice thermal conductivity  $\kappa_L$  (not shown) of the samples is extremely low, of the order of  $0.7$  and  $0.4 \text{ W m}^{-1} \text{ K}^{-1}$  in the perpendicular and parallel directions, respectively. Because of this extremely low thermal transport, Bi does not have a strong influence on  $\kappa_L$ . Of note, these values are significantly lower than those measured in  $\text{Bi}_2\text{Te}_3$ -based alloys but similar to those achieved in  $\alpha\text{-As}_2\text{Te}_3$  or in other chalcogenides.<sup>2,10,22–27</sup> In the parallel direction,  $\kappa_L$  approaches the lowest limit of the thermal conductivity (Figure 2(c)) estimated using the model developed by Cahill and Pohl and the measured longitudinal and transverse sound velocities.<sup>13,28–30</sup>

Figure 2(d), which shows the variations in temperature of the  $ZT$  values, indicates that  $ZT$  increases with temperature for all samples. The peak  $ZT$  of  $0.7$  at  $423 \text{ K}$  achieved in the  $x = 0.017$  sample in the perpendicular direction represents an increase of  $40\%$  compared to the parent compound and evidences the beneficial influence of Bi on the thermoelectric properties of  $\beta\text{-As}_2\text{Te}_3$ . However, due to the narrow compositional range that can be reached in the  $\beta\text{-As}_{2-x}\text{Bi}_x\text{Te}_3$  solid solution, Bi does not push the peak  $ZT$  closer to room temperature. As noted in our prior study,<sup>12</sup> the anisotropy in the electrical resistivity and in the thermal conductivity of  $\beta\text{-As}_{2-x}\text{Bi}_x\text{Te}_3$  does not compensate each other, giving rise to different  $ZT$  values in the parallel and perpendicular directions. Although the hole concentration only slightly changes with the Bi content, the  $ZT$  increases thanks to enhanced power factors achieved at  $423 \text{ K}$  upon Bi alloying.

In summary,  $\beta\text{-As}_2\text{Te}_3$  was found to form a solid solution with  $\text{Bi}_2\text{Te}_3$  in only a narrow compositional window. The alloyed  $\beta\text{-As}_{2-x}\text{Bi}_x\text{Te}_3$  samples are homogeneous up to  $x = 0.035$  as revealed by PXRD and SEM experiments. In this concentration range, the samples behave as heavily doped semiconductors with hole concentrations of the order of  $8 \times 10^{19} \text{ cm}^{-3}$  at  $300 \text{ K}$ . Because the lattice thermal conductivity in  $\beta\text{-As}_2\text{Te}_3$  nears the minimum thermal conductivity, alloying with Bi did not influence significantly the thermal transport. The measured values smoothly decrease below  $1 \text{ W m}^{-1} \text{ K}^{-1}$  at  $423 \text{ K}$  for all samples. The beneficial effect of Bi on the power factor combined with very low thermal conductivity values led to a peak  $ZT$  of  $0.7$  at  $423 \text{ K}$  for  $x = 0.017$  perpendicular to the pressing direction. The complex evolution of the transport properties of  $\beta\text{-As}_2\text{Te}_3$  with the nature of the substituting elements requires further theoretical insights to better understand their influence on the electronic band structure.  $\beta\text{-As}_2\text{Te}_3$  finally appears as an interesting class of compounds that clearly warrants further investigations due to its good thermoelectric performances.

The authors acknowledge the financial support from the French National Agency (ANR) in the frame of its program “PROGELEC” (Verre Thermo-Générateur “VTG”).

<sup>1</sup> H. J. Goldsmid, *Thermoelectric Refrigeration* (Temple Press Books Ltd., London, UK, 1964).

<sup>2</sup> *Thermoelectrics and Its Energy Harvesting*, edited by D. M. Rowe (CRC Press, Boca Raton, FL, 2012).



- <sup>3</sup> T. C. Harman, B. Paris, S. E. Miller, and H. L. Goering, *J. Phys. Chem. Solids* **2**, 181 (1957).
- <sup>4</sup> N. S. Platakis, *J. Non-Cryst. Solids* **24**, 365 (1977).
- <sup>5</sup> Y. Sharma and P. Srivastava, *Opt. Mater.* **33**, 899 (2011).
- <sup>6</sup> T. J. Scheidemantel and J. V. Badding, *Solid State Commun.* **127**, 667 (2003).
- <sup>7</sup> T. J. Scheidemantel, J. F. Meng, and J. V. Badding, *J. Phys. Chem. Solids* **66**, 1744 (2005).
- <sup>8</sup> J. Zhao, L. Yang, Z. Yu, Y. Wang, C. Li, K. Yang, Z. Liu, and Y. Wang, *Inorg. Chem.* **55**, 3907–3914 (2016).
- <sup>9</sup> C. Morin, S. Corallini, J. Carreaud, J.-B. Vaney, G. Delaizir, J.-C. Crivello, E. B. Lopes, A. Piarristeguy, J. Monnier, C. Candolfi, V. Nassif, G. Cuello, A. Pradel, A. P. Gonçalves, B. Lenoir, and E. Alleno, *Inorg. Chem.* **54**, 9936 (2015).
- <sup>10</sup> J.-B. Vaney, J. Carreaud, G. Delaizir, A. Pradel, A. Piarristeguy, C. Morin, E. Alleno, J. Monnier, A. P. Gonçalves, C. Candolfi, A. Dauscher, and B. Lenoir, *Adv. Electron. Mater.* **1**, 1400008 (2015).
- <sup>11</sup> J.-B. Vaney, J. Carreaud, G. Delaizir, C. Morin, J. Monnier, E. Alleno, A. Piarristeguy, A. Pradel, A. P. Gonçalves, E. B. Lopes, C. Candolfi, A. Dauscher, and B. Lenoir, *J. Electron. Mater.* **45**, 1447 (2015).
- <sup>12</sup> J.-B. Vaney, J. Carreaud, G. Delaizir, C. Morin, J. Monnier, E. Alleno, A. Piarristeguy, A. Pradel, A. P. Gonçalves, E. B. Lopes, C. Candolfi, A. Dauscher, and B. Lenoir, *J. Electron. Mater.* **45**, 1786 (2016).
- <sup>13</sup> J.-B. Vaney, J. Carreaud, G. Delaizir, A. Piarristeguy, A. Pradel, E. Alleno, J. Monnier, E. B. Lopes, A. P. Gonçalves, A. Dauscher, C. Candolfi, and B. Lenoir, *J. Mater. Chem. C* **4**, 2329 (2016).
- <sup>14</sup> J.-B. Vaney, J.-C. Crivello, C. Morin, G. Delaizir, J. Carreaud, A. Piarristeguy, J. Monnier, E. Alleno, A. Pradel, E. B. Lopes, A. P. Gonçalves, A. Dauscher, C. Candolfi, and B. Lenoir, “Electronic structure, low-temperature transport and thermodynamic properties of polymorphic  $\beta$ -As<sub>2</sub>Te<sub>3</sub>,” *RSC Adv.* (to be published).
- <sup>15</sup> K. Pal and U. V. Waghmare, *Appl. Phys. Lett.* **105**, 062105 (2014).
- <sup>16</sup> P. Dziawa, B. J. Kowalski, K. Dybko, R. Buczko, A. Szczerbabow, M. Szot, E. Lusakowska, T. Balasubramanian, B. M. Wojek, M. H. Berntsen, O. Tjernberg, and T. Story, *Nat. Mater.* **11**, 1023 (2012).
- <sup>17</sup> T. Liang, Q. Gibson, J. Xiong, M. Hirschberger, S. P. Kodavayur, R. J. Cava, and N. P. Ong, *Nat. Commun.* **4**, 2696 (2013).
- <sup>18</sup> M. Neupane, S.-Y. Xu, R. Sankar, Q. Gibson, Y. J. Wang, I. Belopolski, N. Alidoust, G. Bian, P. P. Shibaev, D. S. Sanchez, Y. Ohtsubo, A. Taleb-Ibrahimi, S. Basak, W.-F. Tsai, H. Lin, T. Dubrakiewicz, R. J. Cava, A. Bansil, F. C. Chou, and M. Z. Hasan, *Phys. Rev. B* **92**, 075131 (2015).
- <sup>19</sup> T. Sato, K. Segawa, K. Kosaka, S. Souma, K. Nakayama, K. Eto, T. Minami, Y. Ando, and T. Takahashi, *Nat. Phys.* **7**, 840 (2011).
- <sup>20</sup> E. Alleno, D. Bérardan, C. Byl, C. Candolfi, R. Daou, R. Decourt, E. Guilmeau, S. Hébert, J. Hejtmanek, B. Lenoir, P. Masschelein, V. Ohorodniichuk, M. Pollet, S. Populoh, D. Ravot, O. Rouleau, and M. Soulier, *Rev. Sci. Instrum.* **86**, 011301 (2015).
- <sup>21</sup> C. Drasar, P. Lostak, and C. Uher, *J. Electron. Mater.* **39**, 2162 (2010).
- <sup>22</sup> S. Sassi, C. Candolfi, J.-B. Vaney, V. Ohorodniichuk, P. Masschelein, A. Dauscher, and B. Lenoir, *Appl. Phys. Lett.* **104**, 212105 (2014).
- <sup>23</sup> C.-L. Chen, H. Wang, Y.-Y. Chen, T. Day, and G. J. Snyder, *J. Mater. Chem. A* **2**, 11171 (2014).
- <sup>24</sup> Q. Zhang, E. Kedebe Chere, J. Sun, F. Cao, K. Dahal, S. Chen, G. Chen, and Z. Ren, *Adv. Energy Mater.* **5**, 1500360 (2015).
- <sup>25</sup> J.-S. Rhyee, K. H. Lee, S. M. Lee, E. Cho, S. Kim, E. Lee, Y. S. Kwon, J. H. Shim, and G. Kotliar, *Nature* **459**, 965 (2009).
- <sup>26</sup> Z.-S. Lin, L. Chen, L.-M. Wang, J.-T. Zhao, and L.-M. Wu, *Adv. Energy Mater.* **25**, 4800 (2013).
- <sup>27</sup> J. H. Kim, M. J. Kim, S. Oh, J.-S. Rhyee, S.-D. Park, and D. Ahn, *Dalton Trans.* **44**, 3185 (2015).
- <sup>28</sup> D. G. Cahill, S. K. Watson, and R. O. Pohl, *Phys. Rev. B* **46**, 6131 (1992).
- <sup>29</sup> D. G. Cahill and R. O. Pohl, *Annu. Rev. Phys. Chem.* **39**, 93 (1988).
- <sup>30</sup> H. Deng, *J. Alloys Compd.* **656**, 695 (2016).